ORIGINAL ARTICLE

Investigation of the effect of the non-stick coating quality on the structure and properties of the surface of cast iron castings

Tatiana Renatovna Gilmanshina[1] · Sergey Alexandrovich Khudonogov[2] · Svetlana Igorevna Lytkina[3] · Angelina Adol`fovna Kovaleva[4] · Dmitry Yurievich Kritsky[4] · Oleg Alexandrovich Masanskii[3] · Alexander Evgenievich Kiselev[4] · Alexander Mikhailovich Tokmin[3] · Inga Anatolievna Kaposko[3]

Abstract

The main objective of the foundry is to produce castings with a surface of high quality, considering the immediate problem involving burn on and surface roughness. An effective way to address the challenge is the creation and application of effective non-stick coatings on the surface of casting molds and cores. For cast iron castings, non-stick coatings based on cryptocrystalline graphites became widely adopted, though not always these graphites ensure iron castings with the adequate surface quality. For the purpose of the study, a self-drying non-stick coating based on natural and mechanically activated cryptocrystalline graphite was selected. The previous studies have shown the results of the effect of mechanical activation modes on the properties of non-stick coatings. This paper investigates the effect of the quality of the non-stick coating on the structure and properties of the surface layer of cast iron castings. The thickening of the cover layer and the thinning down of the penetrating layers have been proven. The dependence of the burn-on value on the wall thickness of the casting and the content of natural and activated graphite in the coating filler on a stepwise test has been investigated. When using coatings based on a mixture of natural and activated graphites, the "heat erosion" defect is not observed, the heat removal from the castings increases, so the transition ferrite layer has lower values. It has been found that the core of all castings is ferrite-pearlite. All samples have demonstrated a propensity to a decrease in microhardness from the periphery to the center. Thus, the application of mixture of natural and activated graphite-bearing coatings allows us to control the structure of the surface layer, which leads to a decrease in burn-on on the surface of ductile iron castings.

Keywords Non-stick coating · Cast iron · Activation · General properties · Technological Properties · Casting mold · Surface of castings

1 Introduction

The main objective of the foundry is to ensure castings with the surface of high quality free from casting defects. In doing this, the immediate problems the manufacturers face with are formation of gritty scale and surface roughness, as the costs involving corrective actions for elimination of defects defects account for 60% of the total labor intensity of their manufacture [1–4].

An effective way to solve this problem is the creation and application of effective non-stick coatings on the surface of casting molds and cores, which would comply with the modern requirements of the foundry, so in view of this, the coatings should [1–6]

✉ Svetlana Igorevna Lytkina
SLytkina@sfu-kras.ru

1   Department of Engineering Bachelor CDIO, Institute of Non-Ferrous Metals and Material Science, Siberian Federal University, Krasnoyarsk 660025, Russia

2   Department of Applied Mechanics, Polytechnic Institute, Siberian Federal University, Krasnoyarsk 660074, Russia

3   Department of Materials Science and Materials Processing Technologies, Polytechnic Institute, Siberian Federal University, Krasnoyarsk 660074, Russia

4   Department of Metal Science and Heat Treatment of Metals Named After V.S. Biront, Institute of Non-Ferrous Metals and Material Science, Siberian Federal University, Krasnoyarsk 660025, Russia

– have a high level of general and technological properties: sedimentation stability, covering power, fire resistance, abrasion resistance, etc.;
– contain refractory filler with a low coefficient of thermal expansion;
– be non-toxic during their manufacture and application on the surface of the mold, as well as not emitting toxic gases during casting into the mold;
– contain no additives which can melt on contact with liquid metal;
– not be gas-generating in contact with liquid metal;
– not form compounds with metal at a low melting point l, its inclusions or oxides;
– be cost effective.

The formation of a high-quality coating layer occurs in two stages (Table 1).

The formation of the properties of non-stick coatings (density, viscosity, sedimentation stability) in the liquid state during the preparation stage occurs due to the proceeding of such physicochemical processes as wettability, adhesive-cohesive interactions, adsorption, absorption, and others [7–10].

The formation of properties in the solid state runs as follows: during drying out, the process of forming the adhesion strength of the coatings on the surface of the casting mold occurs due to the evaporation of water (from aqueous coatings) or solvents (from self-drying coatings).Therefore, the coatings tend to shrink, which result in shrinkage stresses in the coating, thus reducing the adhesion of the coatings to the casting mold. This process in its turn causes cracking and delaminating, which leads to the surface defects of the castings such as burn-ins, scrubbings and cuts [11–17].

The high level of properties of coatings in the liquid state ensures high-quality coating on the surface of the casting mold, and in the solid state during the contact interaction of the melt and the casting mold, it helps to mitigate the formation of defects on the surface of the castings.

The course of the processes in liquid and solid states is determined by the composition of the coating, the method of its application and drying, as well as the state of the surface of the casting mold and the core.

At present, a wide variety of compositions of non-stick coatings have been developed [18–22], though non-stick natural graphite-based coatings used for producing iron castings are the most prevalent. As outlined in the literature, the greatest preference is given to cryptocrystalline graphite [23–25]. However, this graphite does not always ensure the adequate quality of the surface of iron castings on account of the close intergrowth of ash inclusions and graphite particles, as well as the low activity of the particles of the graphite itself.

To solve this problem, special and integrated technologies for the activation of molding materials (including cryptocrystalline graphite) have been developed, coming with deformation of particles, a change in the interplanar distance and crystal system lattice, the formation of a new surface, and a number of other physical and chemical processes that ensure the required properties of non-stick coatings [26–34].

In a number of works, the interrelation of process parameters with molding, quality, microstructure, and properties of castings has been noted [35–37].

Changes in the properties and composition of graphite in terms of activation entail changes in phase transformations that occur in the coating during pouring metal into a casting mold [38, 39].

At the same time, in previous studies, the effect of the quality of non-stick coatings on the structure of the surface layer of cast iron castings has not been studied. This is of particular importance for the castings that are not machined.

Therefore, the purpose of this work is to study the effect of the quality of the non-stick coating on the structure and properties of the surface layer of cast iron castings.

2 Methods of carrying out research

For the research, a self-drying non-stick coating was chosen based on cryptocrystalline graphite from the deposits of the Krasnoyarsk Territory, following 1:1 ratio of graphite to

Table 1 Stages of formation of coatings

Stage of formation of coating property	Processing factors	Properties of the coatings	Physical and chemical factors defining the interaction of coating components
Liquid stage	Composition Mixing method Preparation mode (intensity and time of mixing)	Density, viscosity, sedimentation resistance	Wettability, adsorption, absorbtion, interfacial tension, adhesive and cohesive interaction, electric double layer
Solid stage	Composition Application way (brush, spray) Mold characteristics (mold composition, roughness, porosity, temperature) Drying conditions (temperature, time)	Abrasion resistance, the thickness of coating layer, and the depth of the penetration layer, gas permeability	Filtration of pain through the pores of the mold, cohesive and adhesive force

polyvinyl butyral lacquer. The coating making technology, including the manufacture of varnish by dissolving polyvinyl butyral in alcohol and mixing it with graphite, is described in [40, 41].

The most promising method for improving the quality of graphite is mechanical activation, which was carried out in a planetary-centrifugal mill RETSCH PM 400 MA.

The average particle size of natural graphite (GLS-2) is equal to 60 µm; the mechanically activated graphite (GLS-2A) corresponds to 18 microns. The particle size was determined by the method of light-laser sieving by means of FRITSCHAN ALYSETTE 22 MicroTecPLUS.

The contents of elements of graphites GLS-2 and GLS-2A are given in Table 2 [42].

The phase composition of graphite is represented by graphite, calcite, quartz, cristobalite, pyrite, kaolinite, and illite. Mechanical activation proved not to change the phase composition of graphite.

The quality of the coating was assessed by change in density, abrasion resistance, viscosity, thickness of the coating, and the depth of the penetrating layer.

The density and abrasion resistance of the coatings were assessed according to the methods described in GOST 10,772–78.

The viscosity of the coatings was measured with a VZ-4 viscometer according to the method described in GOST 8420–74.

In order to assess the thickness of the coating and the depth of the penetrating layers, samples were prepared according to GOST 23,409.7–78, intended for studying the tensile strength of wet molding sands. The samples were prepared in a special metal sleeve pipe, after which the coating was applied on the surface of the samples, once the coating has dried the samples were cut to the middle and broken (Fig. 1).
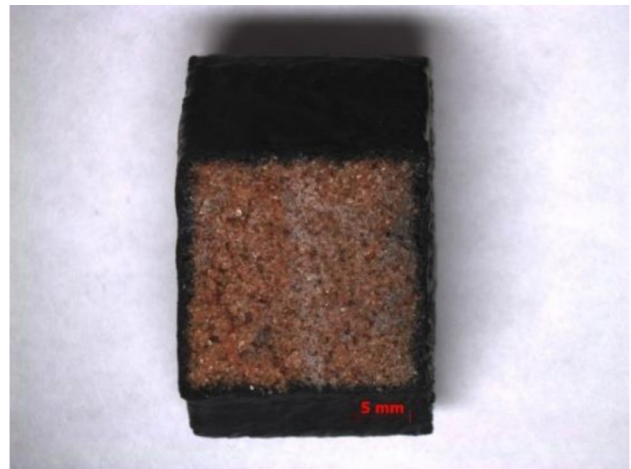

Fig. 1 The sample prepared for measuring the thickness and the depth of the penetrating layers of the coating

The thickness of the cover and the depth of the penetrating layers were studied on the broken side of the sample using the microscope Axio OBSERVER.D1m.

To assess the impact of all factors affecting the formation of defects on the surface of castings, the technological sample must reproduce the real process conditions of the interaction of the surface of the mold with the melt (Fig. 2) [37].

The microstructure was analyzed using a stereomicroscope Stemi 2000-C, and the macrostructure of castings was analyzed using a microscope CarlZeiss AxioOBSERVERT. D1m.
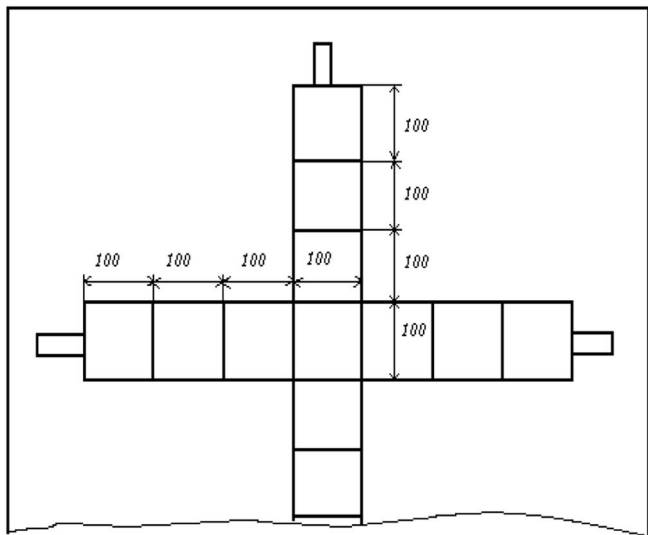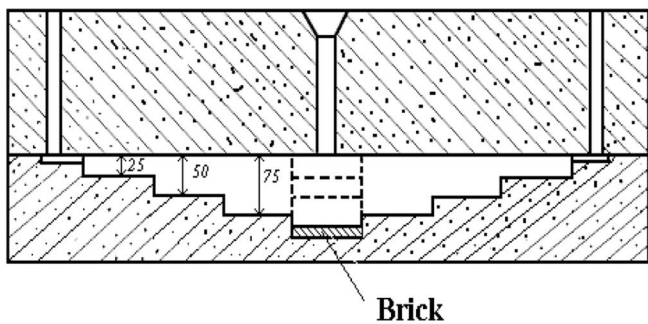
To determine the microhardness of the alloys, a microhardness tester DM8 was used.

3 Research results based on the effect of GLS-2A content on the properties of a non-stick coating

In order to improve the quality of the non-stick coating, it was decided to replace GLS-2 with GLA-2A one partially. The properties of self-drying non-stick composite coatings are given in Table 3 [40, 44].

There has been observed that with an increase in the content of GLS-2A, the density, strength, and abrasion resistance of the coatings increase. In this case, the most significant increase in properties is observed when the content of GLS-2A in the filler is up to 50%. An increase in GLS-2A in the filler from 50 to 100% does not lead to a significant improvement of the properties.

To study the thickness of the cover and the depth of the penetrating layers of self-drying coatings and the thickness of the burn-on one of the surface of the castings, we chose cold-hardening mixtures cured with ester catalysts

Table 2 The content of elements of natural and mechanically activated graphites

Element	The content of elements (%) in graphite	
	Natural graphite (GLS-2)	Mechanically activated graphite (GLS-2A)
Fe	2.10	2.50
Mn	0.08	0.09
Ti	0.17	0.16
Zn	0.02	0.02
Ca	2.4	2.6
K	0.65	0.7
S	0.75	0.7
Si	4.5	3.6
Al	2.6	2.5
Mg	$\leq$0.05	0.8

Fig. 2 The sample to study burn-on on the surface of castings: **a** drawing and **b** appearance [43]

(Alphset-process), the composition of which is presented in Table 4. The samples were coated in one layer with a spray gun and dried in the air.

With an increase in the content of GLS-2A, the density, viscosity, abrasion resistance of coatings, and the depth of

Table 3 Dependence of self-drying non-stick composite coatings properties on the content of GLA-2A in the filler [40, 44]

Content of GLS-2A in filler, %	Property		
	Density, g/cm3	Viscosity, s	Abrasion resistance, g/mm
0	1220	34	175
25	1232	38	180
50	1239	41	187
75	1243	42	189
100	1245	46	190

the penetrating layer of the coating increase, whereas the thickness of the coating layer decreases.

The change in properties can be explained by the fact that particles of GLS-2A graphite have a smaller size than particles of GLS-2 graphite. An increase in the content of GLS-2A graphite in the filler leads to the fact that the coating contains more small particles, providing the coating with a higher density, viscosity, abrasion resistance of coatings, and the depth of the penetrating layer.

In this case, the introduction of 50% of GLS-2A graphite into the filler results in increasing the density by 1.6%, the viscosity by 21%, and the abrasion resistance of the coatings by 7%; a further increase in GLS-2A graphite (up to 100%) leads to an increase in density by 2.0%, viscosity by 35%, and abrasion resistance of coatings by 8%; i.e., no significant increase in properties is observed. Therefore, for further research, we selected a coating, which filler contains 50% of GLS-2 graphite and 50% of GLS-2A graphite.

Table 4 Compositions of cold-hardening mixtures

Component		Properties	
Name	Content, pts. wt	Durability, min	Tensile strength limit (1 h later), MPa
Quartz sand 2K$_1$O$_3$03	100	3.2	0.19
Alfabond resin	2.4		
Hardener T-01	0.4		

4 Research results based on the effect of coating quality on the surface layer structure of cast iron castings

In terms of the research, the following three cases have been studied:

– no coating was applied to the surface of the mold (herein after referred to without coating);
– a coating based on GLS-2 graphite (herein after referred to "GLS-2") was applied to the surface of the mold;
– a coating based on GLS-2 and GLS-2A graphites was applied to the surface of the mold at a ratio of GLS-2 and GLS-2A graphites equal to 50% and 50% (herein after referred to "GLS-2 + GLS-2A").

The coatings were applied to the surface of the mold (Fig. 3), made of a mixture, the composition of which is given in Table 4, according to the model shown in Fig. 2.

The mold was poured with gray cast iron (composition, weight %: C 2.90–2.97; Mn 0.92–0.93; P 0.019–0.021; Si 2.41–2.60; Cu 0.120–0.130; Sn < 0.01; V 0.049–0.052; Ti 0.021–0.024; Ni 0.084–0.086; S 0.042–0.044; Cr 0.100–0.110) at a temperature of 1400 °C.

Investigations of the dependence of the burn-on value on the wall thickness of the casting and the content of GLS-2 and GLS-2A in the coating filler were carried out on a step-wise test (Table 5; Fig. 4).

The minimum thickness for all investigated sections of the casting is observed when using a coating based on a mixture of GLS-2 + GLS-2A.

The thickness of the sticky layer on the bottom of the castings has greater values than on the sides for all investigated sections and non-stick coatings.

In the absence of a non-stick coating on the surface of the castings, there is a "heat cracking" defect (a network of small cracks) arising from the slow heat removal from the casting. The "heat" defect has been detected on all sections under study.

In the heat defect area, the metal is found to be highly oxidized.

Casting metal has ferritic structure with numerous oxide inclusions. Local chill zones are observed in the boundary layer of the casting.

Considering all the findings, it is safe to assume that the process of forming the casting is uncontrollable.

When using GLS-2-based coatings and a mixture of GLS-2 and GLA-2A, the "heat" defect has not been detected.

Fig. 3 Manufacturing technology: **a** bottom half-mold with a model; **b** mold prepared for pouring

Table 5 Burn-on value (the composition of the mixture in Table 4)

Coating base	Section, mm	Burn-on value (μm) on the side of the casting	
		Lateral	Bottom
Without coating	25	68.76–128.18	76.83–199.23
	50	86.44–191.22	123.3–198.22
	75	116.66–251.08	131.84–408.79
GLS-2	25	40.77–66.31	39.88–171.71
	50	60.77–170.81	64.71–265.97
	75	78.77–223.83	82.56–276.84
GLS-2: GLS-2A = 50:50	25	18.97–47.66	22.76–71.13
	50	37.55–49.87	48.41–78.74
	75	50.3–70.18	58.39–131.83

The characteristics of graphite inclusions in casting centre are presented in Fig. 5 and Table 6.

On all castings, surface under investigation the transition layer is visible (Tables 7 and 8; Fig. 6), where the graphite inclusions are smaller compared to those ones of the core.

At the same time, in the surface layer of castings, where the coating was not used, graphite inclusions have a larger size and occupy a smaller area compared with the castings, where the coating was used.

In order to study the metal base of the transition layer, metallographic tests were carried out (Table 9; Fig. 7).

The samples were etched with a 4% solution of nitric acid in alcohol.

The structure of the transition layer of the corner parts casting samples obtained without the use of non-stick coatings and with the use of a non-stick GLS-2 graphite-based coating, for all investigated sections, consists of two layers:

– finely dispersed pearlite layer;
– a mixture of fine pearlite and ferrite with a predominance of ferrite.

The ratio of the thicknesses of these layers is different: with an increase in the thickness of the casting section, the thickness of the structural layer of a mixture of fine pearlite and ferrite is greater (on average by 10–15%).

In the corner part of the castings obtained using a non-stick coating based on a mixture of GLS-2 and GLS-2A, the transition layer consists mainly of fine pearlite and fine granular pearlite, but there are also ferrite segments (Fig. 8).

In castings obtained without the use of a non-stick coating (Sect. 25 mm), a transition layer is observed along the entire length of the casting. While in the castings obtained with the use of coatings based on GLS-2, the transition layer is available only in areas with increased roughness. The presence of a ferrite transition layer on the surface of castings obtained with the use of non-stick coatings based on GLS-2 and GLS-2A was not observed/

For castings with a wall thickness of 50 mm and 75 mm, a transition layer was present for all investigated coatings. The thickness of the transition layer is found to increase with an increase in the wall thickness of the casting from 25 to 75 mm. However, the smallest values of the transition layer were noted for castings obtained with the use of a non-stick coating based on GLS-2 and GLS-2A.

The analysis allows us to assert that at the first stage of the formation of the structure from the liquid, crystallization of austenite begins, then an austenite-graphite eutectic is formed. In the case of accelerated cooling in the interval of eutectoid transformation, austenite turns into pearlite
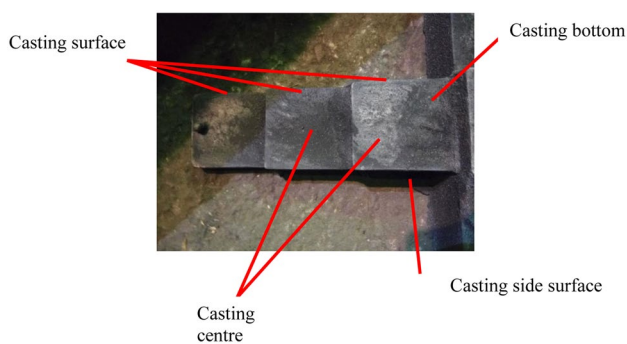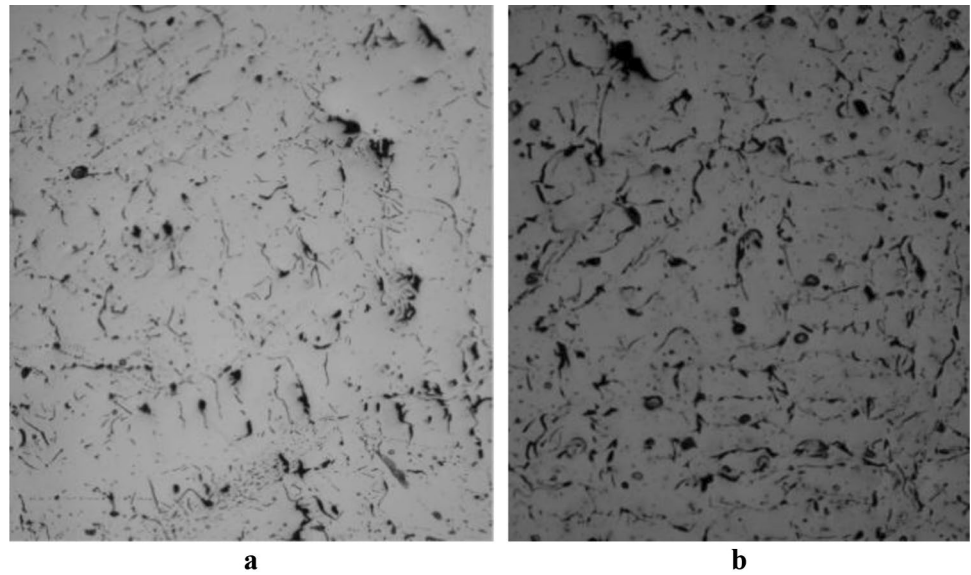

Fig. 4 A fragment of the castings for which coatings were not used

Fig. 5 Microstructure of castings centre (zooming 100×), obtained with the use of coating based on GLS-2 + GLS-2A (casting wall thickness is 25 mm) **a** and without coating (casting wall thickness is 50 mm) **b**

a   b

and gray cast iron on a pearlite base is formed; in the case of delayed cooling, austenite decomposes into ferrite and graphite, and a structure of gray cast iron on a ferritic base is formed.

For the investigated castings, an intermediate case is characteristic, when a part of the austenite decomposes into ferrite and graphite, and part transformed into pearlite; therefore, gray cast iron on a pearlitoferrite base is formed. Elements such as manganese, chromium, nickel, copper, and tin present in the cast iron weaken the iron ferritization process and contribute to the formation of pearlite. Therefore, pearlite predominates in the perlitoferrite mixture.

The formation of ferrite in the transition zone of the casting can probably be explained by the fact that during the course of the eutectoid transformation (at the moment of decomposition of austenite), the rate of heat removal by the mold from the casting is much lower than the rate of heat removal from the central part of the casting to the peripheral one. This hypothesis is confirmed by the fact that graphite inclusions in the transition layer, as shown above, occupy a large surface, while the graphite inclusions themselves are somewhat coarser.

The application of non-stick coatings to the surface of the casting mold increases the heat removal from the castings,

Table 6 Graphite inclusions size in the casting centre

Section, mm	Cover filler	Shape of. graphite inclusions	Length of graphite inclusions, µm	Distribution of graphite inclusions	Squire occupied by graphite, %
25	Without coating GLS-2 GLS-2 + GLS-2A	Laminar straight-lined	60–120	Colonies of lamellar graphite	3–5
50	Without coating GLS-2 GLS-2 + GLS-2A	Laminar straight-lined	120–250	Uniform	< 3
75	Without coating GLS-2 GLS-2 + GLS-2A	Laminar straight-lined	120–250	Uniform	< 3

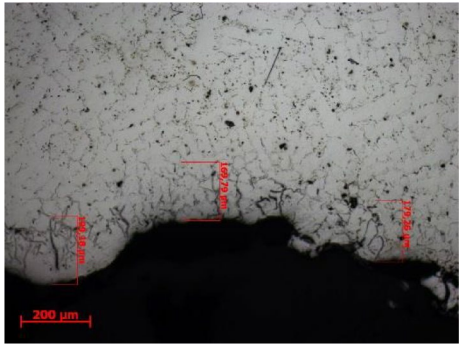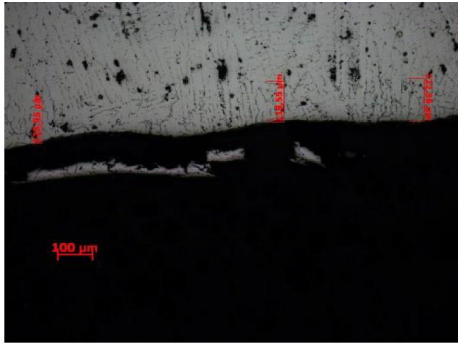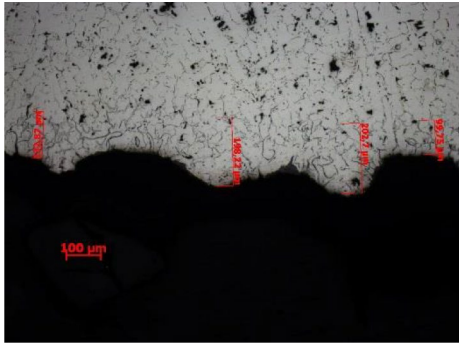**Table 7** Transition layer presented on the surface of cast iron castings
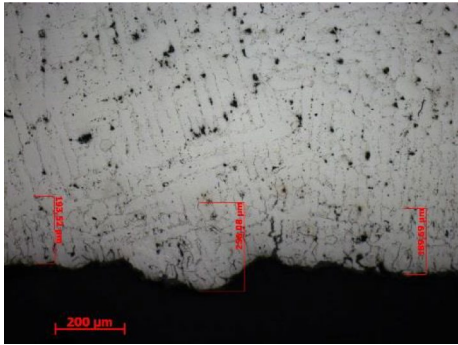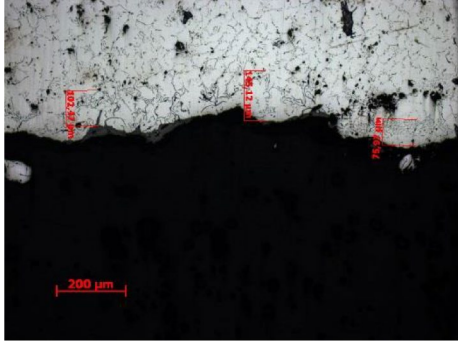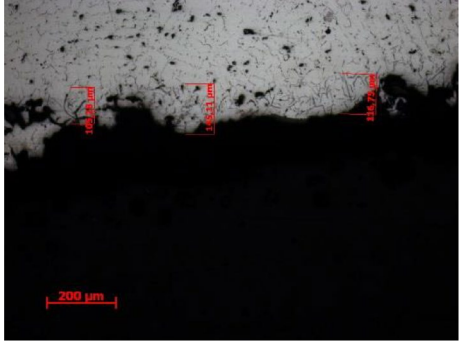
Section thickness, mm	Coating base	Cast surface	
		side	bottom
25	W/o coating		
	GLS-2		
	GLS-2 + GLS-2A		
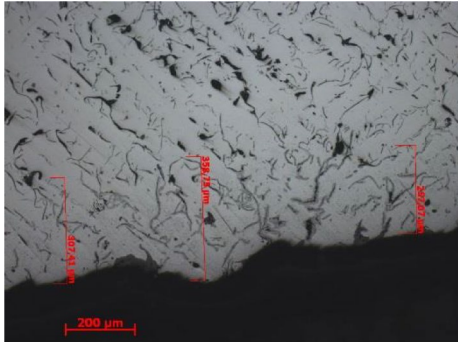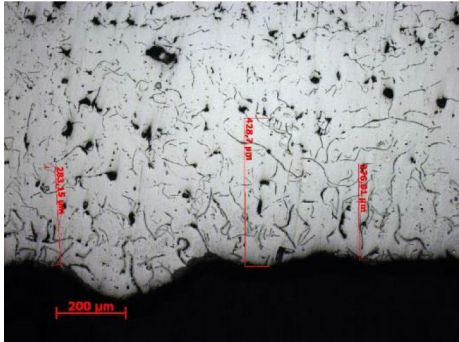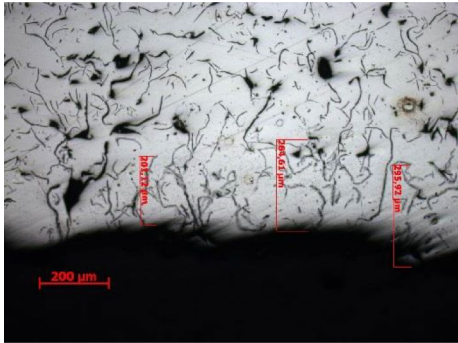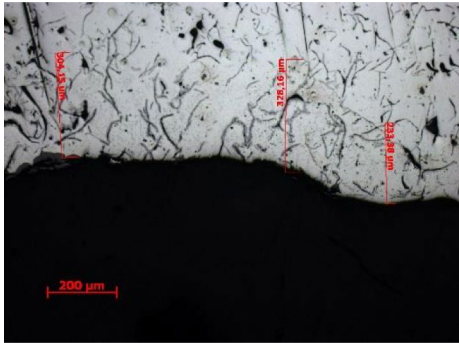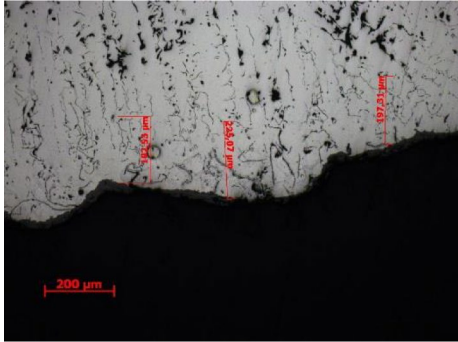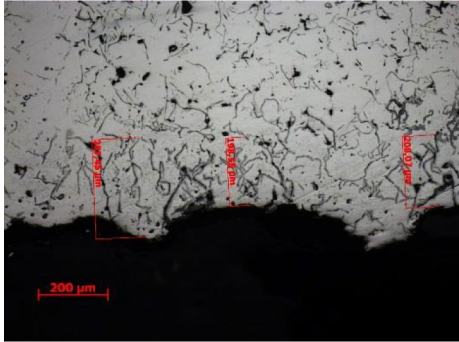
Table 7 (continued)

Section thickness, mm	Coating base	Cast surface	
		side	bottom
50	W/o coating		
	GLS-2		
	GLS-2 + GLS-2A		

Table 7 (continued)
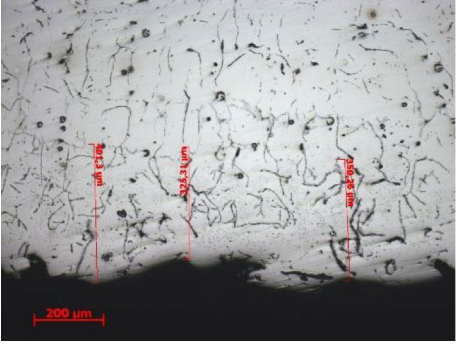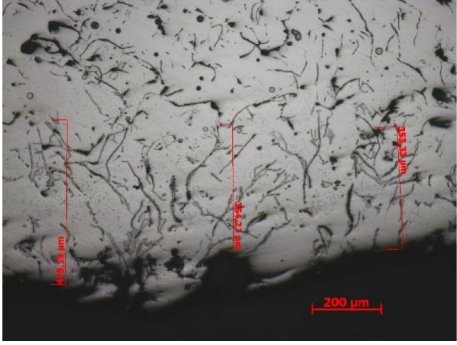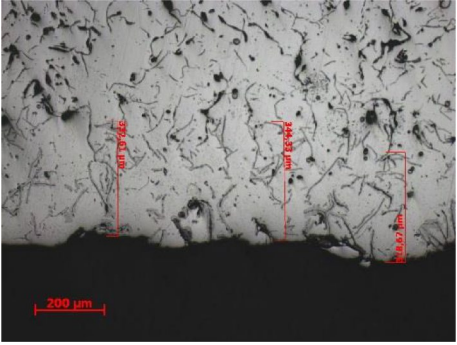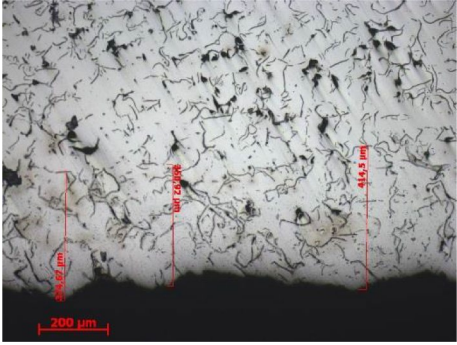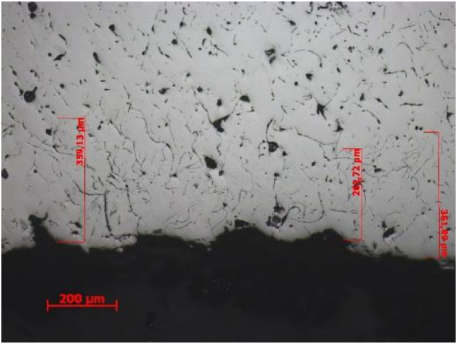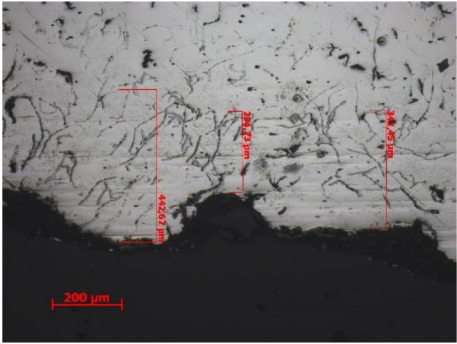
Section thickness, mm	Coating base	Cast surface	
		side	bottom
75	W/o coating		
	GLS-2		
	GLS-2 + GLS-2A		

Table 8 Dimensions of graphite inclusions in the transition layer

Section, mm	Cover filler	Shape of graphite inclusions	Length of graphite inclusions, μm	Distribution of graphite inclusions	Squire occupied by graphite, %
25	Without coating	Laminar exploded	60–120	Colonies of lamellar graphite	3–5
	GLS-2	Laminar exploded	35–60	Colonies of lamellar graphite	5–8
	GLS-2 + GLS-2A	Laminar exploded	35–60	Colonies of lamellar graphite	8–12
50	Without coating	Laminar straight-lined	60–120	Uniform	3–5
	GLS-2	Laminar exploded	60–120	Colonies of lamellar graphite	5–8
	GLS-2 + GLS-2A	Laminar exploded	35–60	Colonies of lamellar graphite	5–8
75	Without coating	Laminar straight-lined	60–120	Uniform	3–5
	GLS-2	Laminar exploded	60–120	Uniform	3–5
	GLS-2 + GLS-2A	Laminar exploded	35–90	Colonies of lamellar graphite	5–8

Fig. 6 Dependence of the transition layer thickness on the castings surface (☐ – bottom; ▨ – side) from the wall thickness of the casting, millimeter: **a** 25; **b** 50; **c** 75
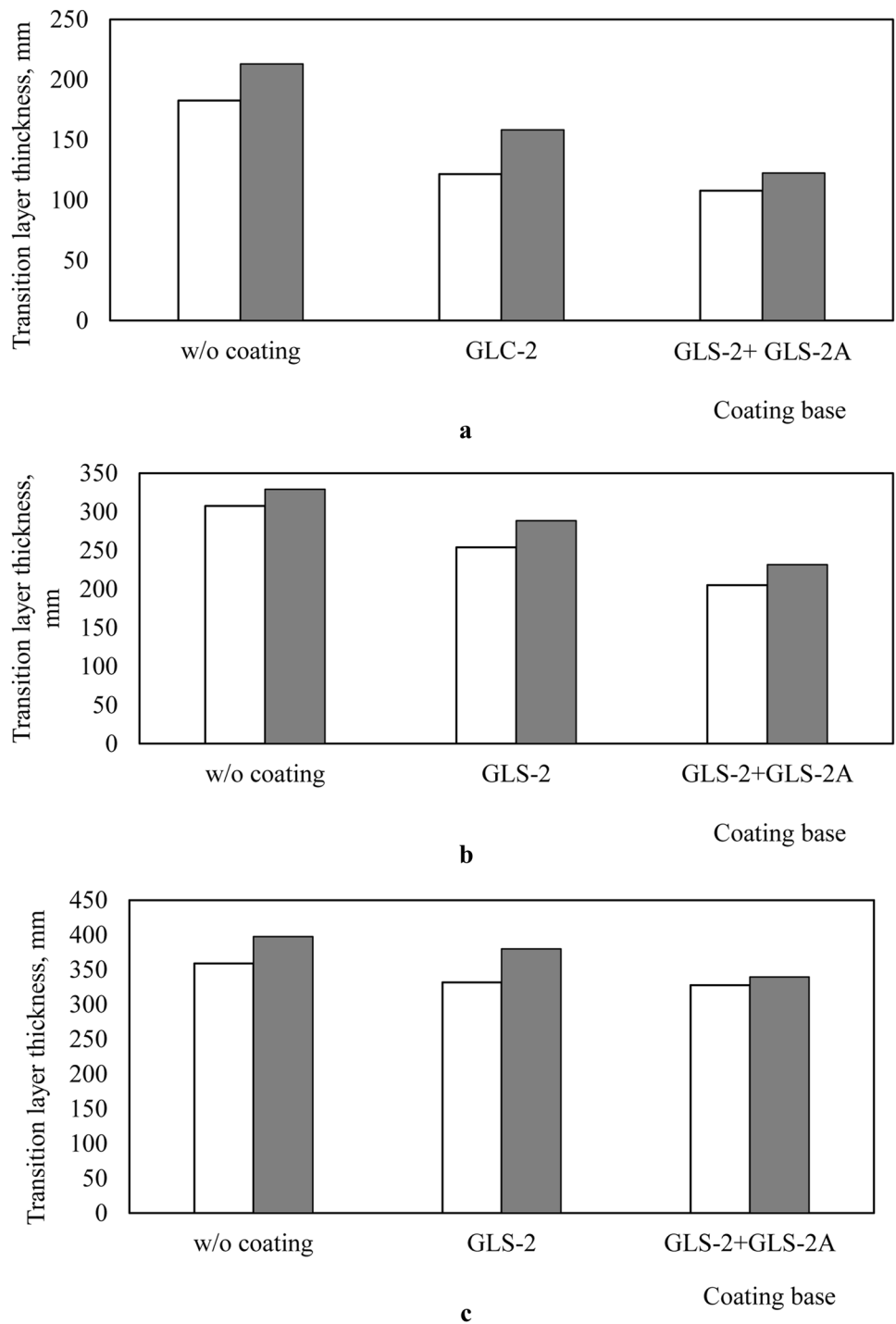

Table 9 Place thickness in grey iron castings (Sect. 25 mm, corner), μm

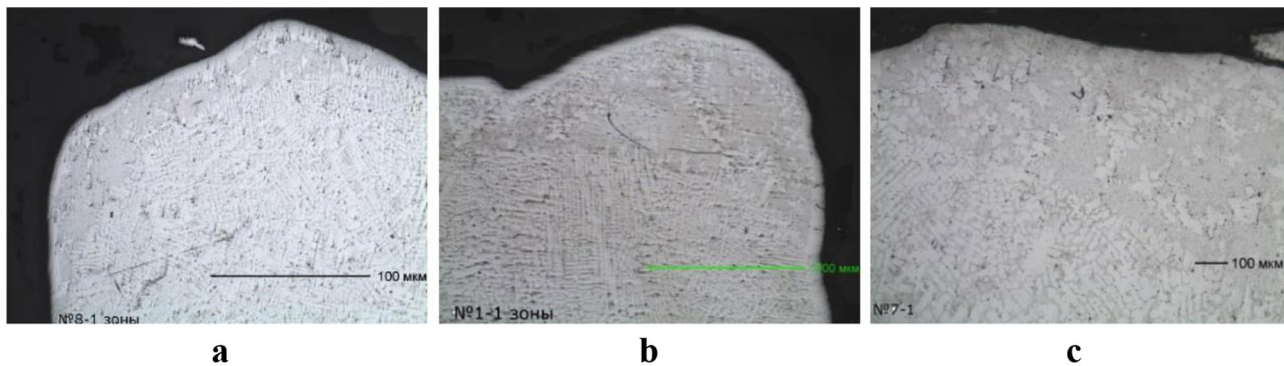| Filler	Place		
	Ferrite layer	Mixtures of fine perlite and fine ferrite	Core
Without coating	10	20	The rest
GLS-2	18	720	
GLS-2:GLS-2A = 50:50	Not detected	500	

Fig. 7 Structure of cast iron castings (Sect. 25 mm, corner part): **a** without coating; coating based on GLS-2 **b** and a mixture of GLS –2 and GLS-2A **c**

Fig. 8 Metallic base of the casting surface layer. The casting mold was coated based on GLS-2 and GLS-2A mixtures
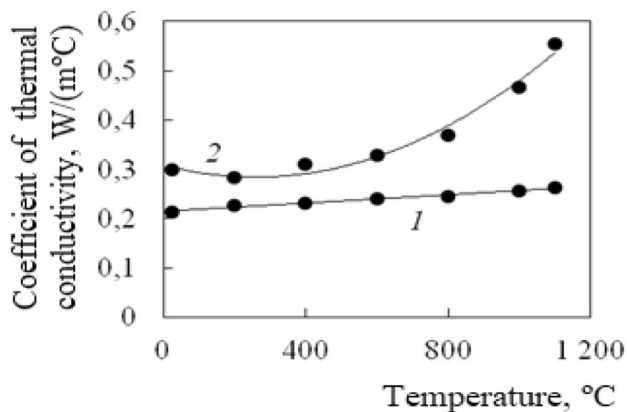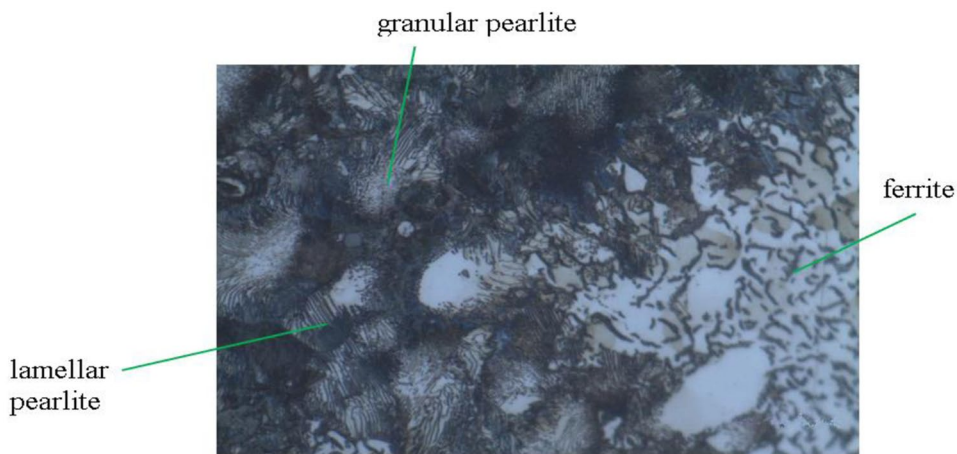

Fig. 9 Thermal conductivity **b** of coatings, containing GLS-2 and GLS-2A with a ratio, *t*. %: 1–100: 0; 2–50: 50 in the filler

which leads to a decrease in the thickness of the transition layer (Fig. 9).
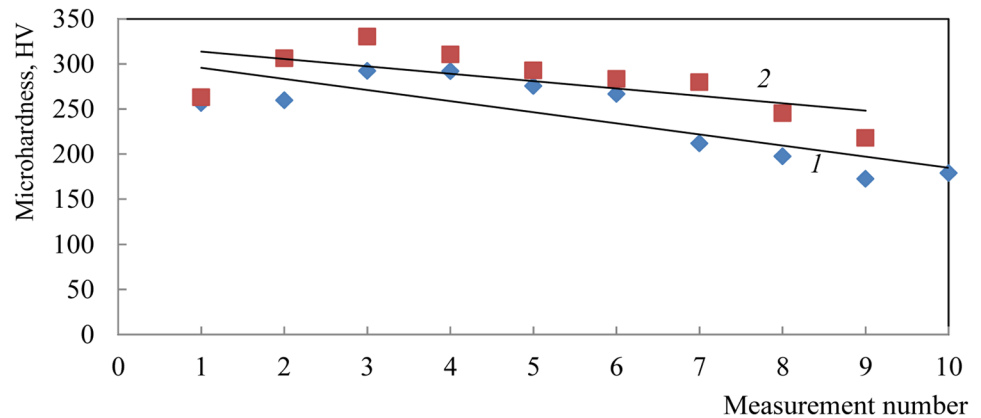
The use of coatings based on a mixture of GLS-2 and GLS-2A to a greater extent increases the heat removal from the castings; therefore, the transition ferrite layer has lower values and the area occupied by graphite has larger values.

Microhardness was measured from the surface to the center of the sample, with a force of 10 MPa. The measurements were made from the edge of the sample with a 2-mm internal (the first 2-mm space from the edge was numbered "1," the second 2-mm space "2," and the other further were numbered, respectively).

The results of measuring the microhardness are shown in Fig. 10.

All samples tend to decrease microhardness from the periphery to the center. The highest average value of

Fig. 10 Microhardness of a sample obtained by means of a coating based on GLS-2 (1) and a mixture of GLS-2 and GLS-2A (2)

microhardness is observed in cast iron obtained in a casting mold, the surface of which is covered by the coating based on a mixture of GLS-2 and GLS-2A. Therefore, this coating has proved to have a positive effect on the microhardness of cast iron SCH20 under investigation.

It has been established that the core of castings (Fig. 11), made without a non-stick coating, using non-stick coatings based on GLS-2 and a mixture of GLS-2 and GLS-2A, was found to have the ferrite-pearlite structure.

Thus, the use of coatings based on a mixture of GLS-2 and GLS-2A makes it possible to control the structure of the surface layer [45].

5 Summary

According to the results, the possibility of improving properties of a self-drying non-stick coating has been shown by partially replacing GLS-2 with GLS-2A one. With an in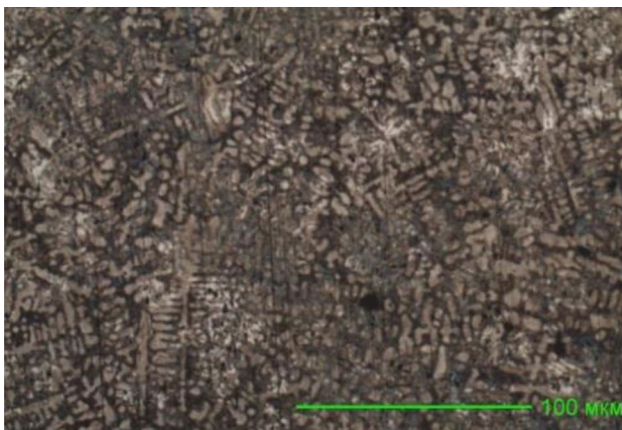crease in the content of GLS-2A graphite in the filler up to 50%, the density of the non-stick coating increases from 1220 to 1245 kg/m^3, the viscosity from 34 to 46 s, the abrasion resistance from 175 to 190 g/μm of the coating, the depth of the penetrating layer from 0.63 to 0.93 mm, and the thickness of the covering layer decreases from 0.46 to 0.06 mm. With a partial replacement of GLS-2 in the filler with an GLS-2A one, particles of GLS-2 form a coating layer, and particles of GLS-2A form a penetrating one. When the metal is poured, the graphite particles are first oxidized from the covering layer with the formation of a reducing atmosphere, and then from the penetrating one. Therefore, the reducing atmosphere appears in the mold cavity from the moment the first portions of the melt arrive and remains in it until the end of the chemical interaction between the metal and mold oxides. This leads to a decrease in burn-on on the surface of gray iron castings by 1.7–3.6 times on the side surfaces of the castings and by 1.2–3.5 times on the bottom surface of the castings, according to the wall thickness of the castings and the type of coating.

In addition, the coatings have high thermal conductivity, which leads to an increase in heat transfer. It results in producing a transition layer on the castings surface, where the graphite inclusions have a smaller size (the size of the graphite inclusions decreases by 1.5–2.0 times) and occupy a large area (by 1.5–2.0 times).

Declarations

Fig. 11 Microstructure of the casting core

References

1. Zenkin RN (2017) Ob ispol'zovanii protivoprigarnyh pokrytij dlya form iz HTS pri poluchenii chugunnyh otlivok. Litejnoe Proizvodstvo 1:11–13

2. Ovcharenko PG, Kuz'minyh EV, Lad'yanov VI (2019) Vzaimodejstvie protivoprigarnogo korundovogo pokrytiya s zhelezouglerodistymi rasplavami v usloviyah lit'ya po gazificiruemym modelyam. Rasplavy 5:469–479

3. Mirzoyan GS, Nuraliev FA, Stepashkin A (2018) Optimizaciya sostava protivoprigarnogo teploizoliruyushchego pokrytiya na vnutrennej poverhnosti izlozhnicy pri centrobezhnom lit'e krupnotonnazhnyh otlivok. Tyazheloe mashinostroenie 6:33–35

4. Cheberyak OI, Chuvagin NF (2017) Tekhnologicheskiye resheniya po ustraneniyu prigara na krupnykh stal′nykh otlivkakh. Liteynoye Proizvodstvo 1:8–10

5. Kashcheev ID, Babkin VG, Mamykin PS, Tsarevskii BV (1973) Kinetic features of fayalite wetting and impregnation of magnesia in isothermal conditions. Refract Ind Ceram 13(3–4):256–259

6. Volkomich AA, Truhov AP, Sorokin A (1996) Formirovanie tochnosti otlivok. M. : MGAATM; AO. Litaform 82

7. Mamina LI (1989) Teoreticheskie osnovy mekhanoaktivacii formovochnyh materialov i razrabotka resursosberegayushchih tekhnologicheskih materialov processov v litejnom proizvodstve: dis. … d-ra tekhn. nauk. Krasnoyarsk 426

8. Illarionov IE, Vasin P (1995) Formovochnye materialy i smesi. CHeboksary: Izd-vo CHuvashaskogo gosudarstvennogo universiteta 2:288

9. Lin Z (2004) Modeling of porosity formation and feeding flow during casting of steel and aluminum alloys. Lin Zhiping [Electron Resour]. Access mode: https://www.researchgate.net/publication/35879052_Modeling_of_porosity_formation_and_feeding_flow_during_casting_of_steel_and_aluminum_alloys

10. Rundman KB (2015) Metal casting: Reference book for MY4130. Dept Mater Sci Eng Michigan Tech Univ 150

11. Aćimović-Pavlović Z, Prstić A, Andrić L et al (2012) Ceramic coating for cast house application [Electron Resour]. Access mode: http://www.issp.ac.ru/ebooks/books/open/Ceramic_Coatings_-_Applications_in_Engineering.pdf

12. Jamrozowicz L, Zych J, Kolczyk J et al (2015) The drying kinetics of protective coatings used on sand molds. Metalurgija 54(1):23–26

13. Romelczyk R, Przyszlak N, Siodmok B et al (2018) The influence of selected water and alcohol based coatings on bending strength of foundry moulds and cores manufactured in furan technology. Arch Found Eng 18(2):169–172. https://doi.org/10.24425/122522

14. Jamrozowicz L, Kolczyk-Tylka J, Siatko A (2018) Investigations of the thickness of protective coatings deposited on moulds and cores. Arch Found Eng 18(4):131–136. https://doi.org/10.24425/afe.2018.125182

15. Jamrozowicz L, Siatko A (2020) The assessment of the permeability of selected protective coatings used for sand moulds and cores. Arch Found Eng 20(1):17–22. https://doi.org/10.24425/afe.2020.131276

16. Di Muoio GL, Tiedje NS (2015) Achieving control of coating process in your foundry. Arch Found Eng 15(4):110–114. https://doi.org/10.1515/afe-2015-0089

17. Rudolph S (2001) Boron nitride release coatings. Alum Cast House Technol 163–170

18. Prstić A, Aćimović-Pavlović Z, Andrić L et al (2012) Zircon-based coating for the applications in lost foam casting process. Chem Ind Chem Eng Quart 18(4):587−593

19. Konrad CH, Brunner M, Kyrgyzbaev K et al (2011) Determination of heat transfer coefficient and ceramic mold material parameters for alloy IN738LC investment castings. J Mater Process Technol 211:181–186

20. Bychkov VP, Osipova NA, Kidalov NA, Zubkova NB (2000) Vysokokoncentrirovannye vodno-glinistye suspenzii. Litejnoe Proizvodstvo 4:20–21

21. Znamenskij LG, Ivochkina OV, Kulakov BA (2006) Elektroimpul'snye nanotekhnologii v litejnyh processah. Litejshchik Rossii 9:8–14

22. Leushin IO, Grachev AN (2002) Razrabotka effektivnyh protivoprigarnyh pokrytij litejnyh form na osnove alyumoshlakovyh napolnitelej. Litejnoe Proizvodstvo 4:13–14

23. Trofimov NV, Leonov AA (2017) Protivoprigarnye pokrytiya, ispol'zuemye dlya form i sterzhnej iz HTS, primenyaemyh pri lit'e magnievyh splavov (obzor). Rezhim Dostupa: http://viam-works.ru/ru/articles?art_id=1193

24. Belyakov AI, Maccarelli D, Belyakov AA, ZHukov AA (2007) Protivoprigarnye pokrytiya dlya form i sterzhnej, primenyaemye pri izgotovlenii otlivok iz chuguna. Zagotovitel'nye Proizvodstva v Mashinostroenii 5:3–10

25. ZHukovskij SS, Anisovich GA, Davydov NI (1993) Formovochnye materialy i tekhnologiya litejnoj formy: Sprav. Pod red. S.S. ZHukovskogo. M.: Mashinostroenie 432

26. Rutkovskaya ES, SHahin IH, Leshchenko SA, Mihajlov F (2019) Aktivaciya grafita v gazodiffuziohhyh elektrodah. Sovremennye elektrohimicheskie tekhnologii i oborudovanie: Mat-ly Mezhdunarodnoj Nauchno-tekhnicheskoj Konferencii 223–227

27. Baklanova ON, Vasilevich AV, Knyazheva OA (2019) Regulirovanie dispersnosti i svojstv poverhnosti uglerodnyh materialov metodom mekhanicheskoj aktivacii: grafit i tekhnicheskij uglerod. Goryachie tochki himii tverdogo tela: ot novyh idej k novym materialam: Mat-ly III Vserossijskoj konferencii s mezhdunarodnym uchastiem, posvyashchennoj 75-letiyu Instituta himii tverdogo tela i mekhanohimii SO RAN: Tezisy dokladov 99

28. Borunova AB, Streleckij AN, Permenov DG, Leonov AV (2015) Vliyanie dozy mekhanicheskoj aktivacii na defektnuyu strukturu iskusstvennogo grafita. Kolloidnyj Zhurnal 77(2):134

29. Mamina LI, Gil'manshina TR, Anikina VI et al (2016) Influence of the activation time on parameters of a graphite structure. Russ J Non-Ferr Metals 57(1):52–56

30. Gilmanshina TR, Lytkina SI, Khudonogov SA et al (2018) Development of the state-of-the-art technologies for improvement of quality of cryptocrystalline graphite. Nanosistemi Nanomateriali Nanotehnologii 16(1):83–101

31. Illarionov IE, Gilmanshina TR, Kovaleva AA, Bratukhina NA (2018) Understanding the effect of structural defects in graphite on the properties of foundry coatings. CIS Iron Steel Rev 16:63–66

32. Amelchenko VN, Illarionov IE, Gilmanshina TR, Borisyuk VA (2018) Graphite as a prospective material for metallurgical application. CIS Iron Steel Rev 16:29–32

33. Gilmanshina TR, Lytkina SI, Zhereb VP, Koroleva GA (2016) Cryptocrystalline graphite chemical-mechanical preparation for subsequent processing stages. Obogashchenie Rud 2(362):14–19

34. Smirnov OM, Krushenko GG, SHCHipko ML (1999) Obogashchenie grafitovoj rudy Kurejskogo mestorozhdeniya. Obogashchenie Rud 1–2:19–22

35. Jiang W, Fan Z, Chen X, Wang B, Wu H (2014) Combined effects of mechanical vibration and wall thickness on microstructure and mechanical properties of A356 aluminum alloy produced by expendable pattern shell casting. Mater Sci Eng A 619(12):228–237

36. Jiang WM, Fan ZT, Liu DJ et al (2012) Influence of process parameters on filling ability of A356 aluminium alloy in expendable pattern shell casting with vacuum and low pressure. Int J Cast Metals Res 25(1):47–52

37. Jiang W, Fan Z, Liu D et al (2013) Effects of process parameters on internal quality of castings during novel casting. Mater Manuf Process 28(1):48–55

38. Babkin VG, Leonov VV, Gilmanshina TR, Stepanova TN (2017) Phase transformations in graphite coatings and their effect on surface cleanness of castings. Chernye Met 10:54–59

39. Gilmanshina TR, Illarionov IE, Kovaleva AA, Lytkina SI (2019) Water-based antiburning coatings for iron castings. Chernye Met 10:18–22

40. Gilmanshina TR, Perfilyeva NS, Illarionov IE, Zhirkov EN (2020) Study of the dependence of non-stick coatings properties on the mode of mechanical activation of graphites. Chernye Met 2:21–25

41. Illarionov IE, Gilmanshina TR, Kovaleva AA, Borisyuk VA (2019) Study of the depth of penetration of self-heating non-stick coatings in cold-hardening mixtures. Chernye Met 1:21–25

42. Gilmanshina TR, Koroleva GA, Baranov VN, Kovaleva AA (2017) The Kureyskoye deposit graphite mechano-thermochemical modification technology. Obogashchenie Rud 4:7–11

43. Illarionov IE, Kaftannikov AS, Nuraliev FA, Gilmanshina TR (2018) Evaluation of burn value on the surface of iron castings. Chernye Met 8:23–28

44. Gilmanshina TR, Khudonogov SA, Lytkina SI, Perfilyeva NS (2020) Choice of the optimal composition of non-stick coatings according to the conditional criterion of filling mass activation. CIS Iron Steel Rev 19:23–26

45. Kolokol'cev VM, Vdovin KN, Kuc VA (1997) Abrazivnaya iznosostojkost' lityh stalej i chugunov. M.: MiniTip (Magnitogorsk) 148